Simple dynamical system with discrete bound states

Jayme De Luca
Departamento de Física, Universidade Federal de São Carlos, Rodovia Washington Luiz, km 235, Caixa Postal 676, São Carlos, São Paulo 13565-905, Brazil
(Received 2 March 2000; revised manuscript received 26 April 2000)

We study numerically the dynamical system of a two-electron atom with the Darwin interaction as a model to investigate scale-dependent effects of the relativistic action-at-a-distance electrodynamics. This dynamical system consists of a small perturbation of the Coulomb dynamics for energies in the atomic range. The key properties of the Coulomb dynamics are (i) a peculiar mixed-type phase space with sparse families of stable nonionizing orbits and (ii) scale-invariance symmetry, with all orbits defined by an arbitrary scale parameter. The combination of this peculiar chaotic dynamics [(i) and (ii)], with the scale-dependent relativistic corrections (Darwin interaction), generates the phenomenon of scale-dependent stability: We find numerical evidence that stable nonionizing orbits can exist only for a discrete set of resonant energies. The Fourier transform of these nonionizing orbits is a set of sharp frequencies. The energies and sharp frequencies of the nonionizing orbits we study are in the quantum atomic range.

PACS number(s): 05.45.Pq, 31.15.Ct, 45.05.+x

I. INTRODUCTION

The Coulomb dynamical system of the helium atom is a very peculiar chaotic system that exhibits Arnold diffusion [1], and with a typical trajectory having an infinity of possible time-asymptotic final states. For example, almost all negative-energy trajectories of Coulombian helium display the generic phenomenon of ionization, namely, the ejection of one electron [2,3]. Several nonlinear dynamical systems share this property of having more than one time-asymptotic final state, with the respective basins for each outcome having a complicated structure in initial condition space [4,5]. The numerical work in this paper is based on stable Coulombian orbits of a two-electron atom that do not ionize for several millions of turns of one electron around the nucleus. It is a property of the Coulomb dynamics of a two-electron atom that most initial conditions with a negative energy ionize very quickly in about 20 turns [2,3]. Then there are the very special initial conditions that do not ionize due to a precise phase balance between the two electrons. These rare nonionizing orbits are defined very sharply in phase space and were first studied in Refs. [2] and [3] for plane orbits. Here we also develop a numerical procedure to search for nonionizing orbits among a large number of possible tridimensional initial conditions.

The Coulomb Hamiltonian exhibits the scale-invariance degeneracy: if we scale time and space as $t \to Tt$, $\vec{r} \to L\vec{r}$, the equations of motion are left invariant if $T^2/L^3 = 1$ (this simple scale relation is Kepler's third law of gravitation). For this reason, the behavior of the Coulomb dynamics is the same in all scales, a degeneracy which is broken by the relativistic effects of electrodynamics. The phenomenon of breaking the scale invariance in electrodynamics was explored analytically in [6,7] for the Darwin interaction, which is the low-velocity approximation to the Wheeler-Feynman action-at-a-distance electrodynamics [8]. It was found in [6,7] that a simple resonant normal form approximation theory predicts a discrete set of quantized scales very close to the quantum atomic energies. Using these preliminary findings as a guide, we present a numerical investigation of the stability of nonionizing orbits for the Darwin dynamics and its dependence on the energy scale. It turns out that for energies of atomic interest, the Darwin equations of motion approximate the Coulomb equations plus a perturbation of size β^2, with $\beta \sim 10^{-2}$. Therefore, nonionizing stable orbits of the Darwin dynamics should exist in the neighborhood of nonionizing stable Coulombian orbits if the perturbation does not force ionization. For these, our numerical results with Darwin dynamics indicate that the nonionizing property plus stability requires sharply defined discrete energies.

This paper is organized as follows: In Sec. II we discuss how the Darwin Hamiltonian can be an approximation to a time-reversible direct-interaction relativistic physical theory. In Sec. III we describe the numerical calculations with the Coulomb limit of the Darwin interaction, and find some nonionizing orbits and their Fourier transforms. In Sec. IV we include the scale-dependent Darwin terms and investigate the possibility of stable nonionizing orbits. In Sec. V we give the conclusions and discussion.

II. DIRECT-INTERACTION ELECTRODYNAMICS

The Darwin interaction is not exactly a Lorentz invariant interaction [9–11], so we study it as an approximation to the relativistic action-at-a-distance electrodynamics, for the sake of including the present approach into an underlying physical theory. Maxwell's theory would seem to be the natural candidate for the comprehensive physical theory, but it lacks time reversibility and dipolar dissipation would forbid the orbits studied in this paper. In the face of this, an alternative physical theory would be a direct-interaction theory. This theory could be the Wheeler-Feynman action-at-a-distance electrodynamics, for example [12], and in fact the Darwin interaction is the low-velocity approximation to the Wheeler-Feynman electrodynamics [8].

Wheeler and Feynman showed that electromagnetic phenomena can be described by the action-at-a-distance electrodynamics in complete agreement with Maxwell's electrodynamics as far as the classical experimental consequences [12,13]. This direct-interaction formulation of electrodynamics was developed to avoid the complications of a divergent self-interaction, as there is no self-interaction in the theory, and also to eliminate the infinite number of field degrees of freedom of Maxwell's theory [14] (and there is no loose radiation in the theory either). It was a great inspiration of Wheeler and Feynman in 1945 [12] that showed, with the extra hypothesis that the electron interacts with a completely absorbing universe, that the advanced response of this universe to the electron's retarded field arrives *at the present time of the electron* and is equivalent to the local instantaneous self-interaction of the Lorentz-Dirac theory [15]. The action-at-a-distance electrodynamics is symmetric under time reversal, and dissipation is only due to interaction with the other charges of the universe and becomes a matter of statistical mechanics of absorption [16] (the Lorentz-Dirac dissipation being just a special limiting way of interaction with the other charges of the universe [12]). In this paper we are only interested in the nondissipative isolated two-electron system.

In the following we resort to the Darwin approximation not as much as a mathematical approximation to the action-at-a-distance electrodynamics, but as a physical approximation of Lorentz-invariant direct-interaction dynamics in the atomic shallow-energy range. There are today several choices of direct-interaction Lorentz-invariant systems, either Lagrangian [17] or constrained Hamiltonian dynamical systems [18–21], whose exact forms are actually more amenable to numerical treatment than the Wheeler-Feynman electrodynamics, but we shall not discuss them here.

III. NUMERICAL CALCULATIONS FOR THE COULOMB DYNAMICS

To introduce our numerical calculations, we start from the scale-invariant Coulomb limit of the Darwin interaction: Let $-e$ and m be the electronic charge and mass, respectively, and Ze the nuclear charge of our two-electron atom. The nucleus is assumed infinitely massive and resting at the origin. Our numerical work uses a scaling that exploits the scale invariance of the Coulomb dynamics: Given a negative energy, there is a unique circular orbit at that energy with frequency ω_o and radius R related by $e^2/(m\omega_o^2 R^3)=1/(Z-\frac{1}{4}) \equiv \zeta(Z)$. We scale distance, momentum, time, and energy as $x \to Rx$, $p \to m\omega_o R p$, $\omega_o dt \to d\tau$, and $E \to m\omega_o^2 R^2 \hat{H}$, respectively. In these scaled units, the Coulomb dynamics of the two-electron atom is described by the scaled Hamiltonian

$$\hat{\mathbf{H}}=\frac{1}{2}(|\vec{p}_1|^2+|\vec{p}_2|^2)+\zeta(Z)\left\{\frac{1}{r_{12}}-\frac{Z}{r_1}-\frac{Z}{r_2}\right\}, \qquad (1)$$

where $r_1 \equiv |\vec{x}_1|$, $r_2 \equiv |\vec{x}_2|$, $r_{12} \equiv |\vec{x}_1 - \vec{x}_2|$ (single bars represent Euclidean modulus), and $\beta \equiv \omega_o R/c$. For a generic noncircular orbit, β plays the role of a scale parameter, and we recover the value of the energy in ergs through $E = mc^2\beta^2\hat{H}$. Notice that β does not appear in the scaled Hamiltonian, which is the scale-invariance property. From the scaled frequency $\hat{w}$ and scaled angular momentum $\hat{l}$ we can recover the actual values in cgs units by the formulas

$$w=\frac{mc^2\zeta(Z)\beta^3}{e^2/c}\hat{w}, \quad l=\frac{e^2/c}{\zeta(Z)}\frac{\hat{l}}{\beta}. \qquad (2)$$

The only other analytic constant of the Coulomb dynamics, besides the energy (1), is the total angular momentum, and this dynamics is chaotic and displays Arnold diffusion, as proved in [1] for a similar three-body system.

Our numerical calculations were performed using a ninth-order Runge-Kutta embedded integrator pair [22]. We chose the embedded error per step to be 10^{-14}, and after 10×10^6 time units of integration the changes in energy and total angular momentum were less than 1 part in 10^6. As a numerical precaution we performed the numerical calculations using the double Kustanheimo coordinate transformation to regularize single collisions with the nucleus [23]. As these alone are not enough for faithful integration, we checked that there was never a triple collision, as the minimum interelectronic distance was about 0.3 units while the minimum distance to the nucleus was 0.01 units for all the orbits considered in this work. We also checked that along stable nonionizing orbits we can integrate forward up to 50 000 time units, reverse the integration, go backwards another 50 000 units, and recover the initial condition with a percentile error of 10^{-5}. (Notice that the embedded integrator will not repeat the same exact forward steps in the backwards integration.) For longer times this precision of back and forth integration degenerates rapidly, which is due to the combined effect of numerical truncation and stochasticity. The question of how far in time the numerical trajectories approximate shadowing trajectories in the present system is far from trivial [24], but we assume it to be a time at least of the order of these 100 000 units. (Energy conservation of 1 part in 10^6 is achieved for much longer times, even 1×10^8 time units.)

The study of orbits of a two-electron atom was greatly stimulated by the recent interest in semiclassical quantization, and these studies discovered two types of stable zero-angular-momentum periodic orbits for helium ($Z=2$): the Langmuir orbit and the frozen-planet orbit [25,26]. A detailed study of the nonionizing orbits of Coulombian helium was initiated in Refs. [2] and [3] for plane orbits, and we describe some of their results below. There are basically two types of nonionizing orbits: symmetric if $r_1=r_2$ for all times and asymmetric if $r_1 \neq r_2$ generically. Symmetric orbits are produced by symmetric initial conditions like, for example, $\vec{x}_1(0)=-\vec{x}_2(0)$ and $\vec{p}_1(0)=-\vec{p}_2(0)$ or $\vec{x}_1(0)=-\vec{x}_2(0)$ and $\vec{p}_1(0)=\vec{p}_2(0)$ with $\vec{x}_1(0)\cdot\vec{p}_1(0)=0$ [25]. Because Eq. (1) is symmetric under particle exchange, these orbits satisfy $r_1=r_2$ at all times, and therefore cannot ionize if $H<0$ (both electrons would have to ionize at the same time, which is impossible at negative energies). For example the double-elliptical orbits (two equal ellipses symmetrically displaced along the x axis) discussed in [7] are in this class. Double-elliptical orbits are known to be unstable [6,7] and we find that they ionize in about 100 turns because of the numerical truncation error. Most symmetric plane orbits are very un-

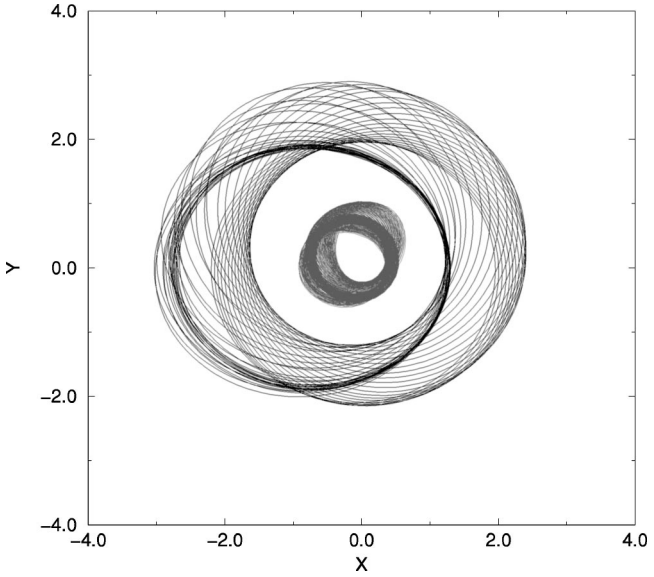

FIG. 1. Nonionizing double-ring orbit for a Ca^{+18} ion ($Z=20$), obtained from the initial condition $\vec{x}_1=(r_1,0,0)$, $\vec{p}_1=(0,v_1\sqrt{4/7},0)$, $\vec{x}_2=(-1.0,0,0)$, $\vec{p}_2=(0,-\sqrt{4/7},0)$, with $r_1=1.4$ and $v_1=1.28442$. Trajectories are shown for the first 900 time units, the inner ring represents the orbit of electron 1, and the outer ring represents the orbit of electron 2. Positions are measured in the scaled units defined in Sec. III.

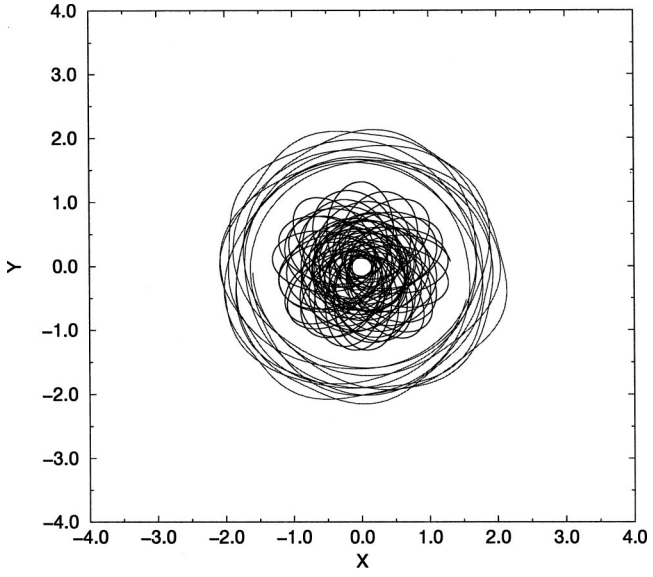

FIG. 2. Nonionizing double-ring tridimensional orbit for helium ($Z=2$). Trajectories are shown for the first 200 time units, the inner ring represents the plane projection of the orbit of electron 1, and the outer ring represents the projection of the orbit of electron 2. Positions are measured in the scaled units defined in Sec. III.

stable to asymmetric perturbations, with the exception of the Langmuir orbit for a small range of Z values around $Z=2$ [25].

The simplest way to produce an asymmetric nonionizing plane orbit is from the initial condition $\vec{x}_1=(r_1,0,0)$, $\vec{p}_1=(0,v_1\sqrt{4/7},0)$, $\vec{x}_2=(-1.0,0,0)$, $\vec{p}_2=(0,-\sqrt{4/7},0)$, as suggested in [2,3]. In Fig. 1 we show the electronic trajectories for the first 300 scaled time units along a two-dimensional nonionizing orbit of $Ca^{18+}(Z=20)$ with $r_1=1.4$ and $v_1=1.284\,42$ in the above-defined condition. We used a numerical refining procedure to finely adjust v_1 so as to maximize the nonionizing time and this condition of Fig. 1 does not ionize for 5×10^4 time units. The orbit survives that far only for a very sharp band of values of v_1, other neighboring values producing quick ionization. This orbit was named a double-ring torus in [2,3]. The other possible type of nonionizing orbit resulting from the above initial condition, depending on (r_1,v_1), is what was named a braiding torus in Refs. [2,3], with both electrons orbiting within the same region. A search over (r_1,v_1) was conducted in [3], and it was found that most values of (r_1,v_1) produce quick ionization except for a zero-measure set of (r_1,v_1) values where braiding tori or double-ring orbits are found. This suggests the general result that nonionizing orbits are rare in phase space.

To search for general tridimensional nonionizing orbits in phase space, it is convenient to introduce canonical coordinates $\vec{x}_d$ and $\vec{x}_c$:

$$\vec{p}_d\equiv(\vec{p}_1-\vec{p}_2)/\sqrt{2},\quad \vec{x}_d\equiv(\vec{x}_1-\vec{x}_2)/\sqrt{2},$$
$$\vec{p}_c\equiv(\vec{p}_1+\vec{p}_2)/\sqrt{2},\quad \vec{x}_c\equiv(\vec{x}_1+\vec{x}_2)/\sqrt{2}. \tag{3}$$

Initial conditions with $\vec{x}_c=\vec{p}_c=0$ and with a negative energy describe double-elliptical orbits (and circular as a special case). To describe a generic elliptical orbit we exploit the scale invariance and set the energy to -1. It is then easy to check that elliptical orbits of the Hamiltonian (1) with an energy of -1 must have a total angular momentum of magnitude ranging from 0 to 2. To exploit the rotational invariance of Eq. (1), we can choose the plane defined at $\vec{x}_c=\vec{p}_c=0$ by the angular momentum $\vec{L}=\vec{x}_d\times\vec{p}_d+\vec{x}_c\times\vec{p}_c=\vec{x}_d\times\vec{p}_d$ to be the xy plane. On this xy plane a single number $0<|\vec{x}_d\times\vec{p}_d|<2$ (the angular momentum) determines completely the elliptical orbit. The next step in producing a generic orbit is to add all possible perturbations along $\vec{x}_c$ and $\vec{p}_c$ to the chosen elliptical orbit. These are six numbers, and once we are looking for bound oscillatory orbits, we can choose $z_c=0$, once z_c has to cross the xy plane at some point, so we need five independent numbers for each angular momentum of an elliptical orbit seed, which totals six parameters. Our numerical search procedure consists in varying these six parameters over a fine grid, integrating every single initial condition until the distance from one electron to the nucleus is greater than 20 units, which is our ionization criterion. This criterion fails if the orbit has a very low angular momentum because these can go far away from the nucleus and come back, and therefore our search possibly misses low-angular-momentum nonionizing orbits. As the majority of the initial conditions ionize very quickly, this search procedure is reasonably fast. We first perform a coarse search for ionization times above 1000 units and then refine in the neighborhood of each surviving condition to get conditions that do not ionize after 1×10^6 time units.

Using the above numerical search procedure we found the tridimensional nonionizing initial condition of Fig. 2 for helium, a tridimensional double-ring orbit generated by the initial condition

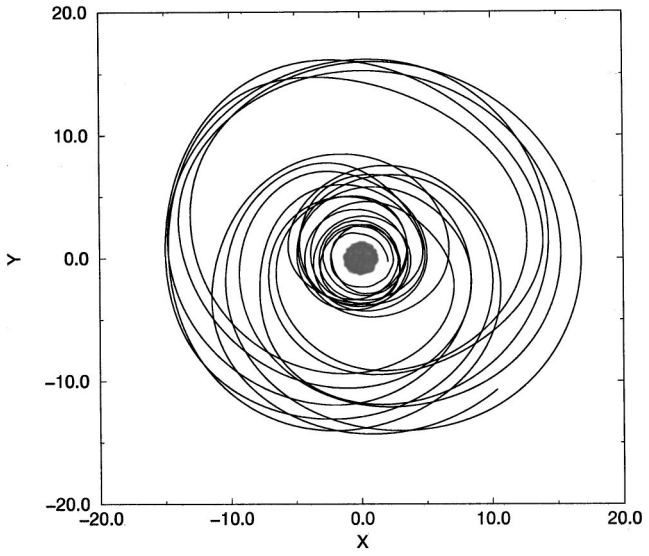

FIG. 3. Nonionizing tridimensional orbit for H^- ($Z=1$). Trajectories are shown for the first 10 000 time units. The inner ring represents the plane projection of the orbit of electron 1 and the outer ring represents the projection of the orbit of electron 2. Trajectory of the (fastest) electron 1 winds almost everywhere in the the dark inner core of the figure. Positions are measured in the scaled units of Sec. III.

$$\vec{x}_1=(1.2812617,0.0147169,0.0),$$

$$\vec{x}_2=(-1.5511484,0.0147169,0.0),$$

$$\vec{p}_1=(-0.0194868,0.4398889,0.1094930),$$

$$\vec{p}_2=(-0.0194868,-0.7972467,0.1094930),$$

which does not ionize before 10×10^6 turns. (After the search and refinement, we scaled this orbit's energy to -1, for later convenience.) We also found the nonionizing orbit orbit of Fig. 3 for H^- ($Z=1$), a tridimensional orbit generated by the condition

$$\vec{x}_1=(1.9776507,-0.3411364,0.0),$$

$$\vec{x}_2=(-1.2288121,-0.3411364,0.0),$$

$$\vec{p}_1=(0.0421302,0.5057782,0.2810539),$$

$$\vec{p}_2=(0.0421302,-0.4132970,0.2810539),$$

which does not ionize before 1×10^6 turns. (The Coulombian energy of this condition is also -1.) This last orbit is fragile and numerically harder to find: as the first electron has an orbit very close to the positive $Z=1$ charge, there remains only a dipole field to bind the second electron. As the outer electron is much slower in the scaled units, we had to plot the first 10 000 time units of evolution to display the generic features of the trajectory. Nonionizing orbits of H^- are very rare in phase space, which is reminiscent of the quantum counterpart, as the H^- ion is known to have only one quantum bound state at $E\simeq-0.55mc^2\alpha^2$, very close to the ionization threshold ($-0.5mc^2\alpha^2$) [27].

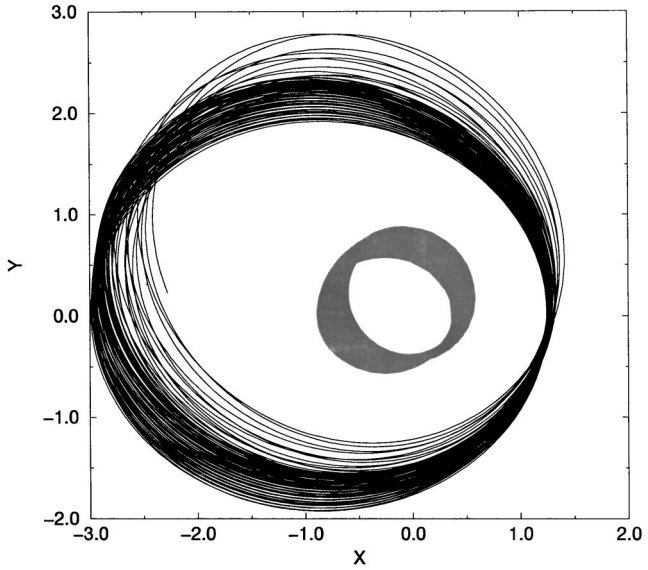

FIG. 4. Nonionizing double-ring orbit for Zr^{+38} ($Z=40$), obtained from the initial condition $\vec{x}_1=(r_1,0,0)$, $\vec{p}_1=(0,v_1\sqrt{4/7},0)$, $\vec{x}_2=(-1.0,0,0)$, $\vec{p}_2=(0,-\sqrt{4/7},0)$, with $r_1=1.4$ and $v_1=1.3123$. Trajectories are shown for the first 2000 time units, the inner ring represents the orbit of electron 1, and the outer ring represents the orbit of electron 2. Positions are measured in the scaled units defined in Sec. III.

A last nonionizing condition we consider is an asymmetric plane orbit for the case $Z=40$, which is generated from the initial condition $\vec{x}_1=(r_1,0,0)$, $\vec{p}_1=(0,v_1\sqrt{4/7},0)$, $\vec{x}_2=(-1.0,0,0)$, $\vec{p}_2=(0,-\sqrt{4/7},0)$, with $r_1=1.4$ and $v_1=1.3123$. In Fig. 4 we show the electronic trajectories for the first 2000 scaled time units along this two-dimensional nonionizing orbit. As Z becomes large, the electronic interaction becomes a small perturbation to the inverse-square central force, and the orbit of Fig. 4 is approximately two ellipses with some precession due to the small electronic interaction (the two ellipses are in the same plane).

One remarkable fact about these nonionizing orbits is that they all have a very sharp Fourier transform. This property makes them approximately quasiperiodic orbits. For example, in Fig. 5 we plot the fast Fourier transform of the orbit of Fig. 2, performed using 2^{16} points. (It seems that there are at least two basic frequencies in the resonance structure of Fig. 5.) Even though these orbits look like quasiperiodic tori, there seems to be a thin stochastic tube surrounding each orbit, as evidenced by a small positive maximum Lyapunov exponent. We calculated numerically this maximum Lyapunov exponent by doubling the integration times up to $T=10^7$ and found that the exponent initially decreases but then saturates to a value of about 0.001 for the orbits of Figs. 1, 2, and 3. The gravitational three-body problem has recently been proved to display Arnold diffusion [1], and this numerically calculated positive Lyapunov exponent suggests that the same is true for the two-electron Coulombian atom.

IV. NUMERICAL CALCULATIONS FOR THE DARWIN DYNAMICS

The numerical integrations in this section are performed with the vector field of the Darwin Hamiltonian approxima-

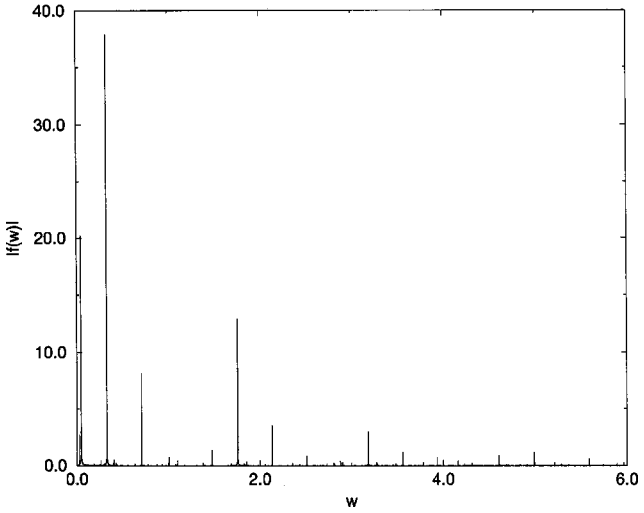

FIG. 5. Fast Fourier transform of the orbit of Fig. 2 using 2^{16} points. Frequencies are measured in the scaled units of Sec. III.

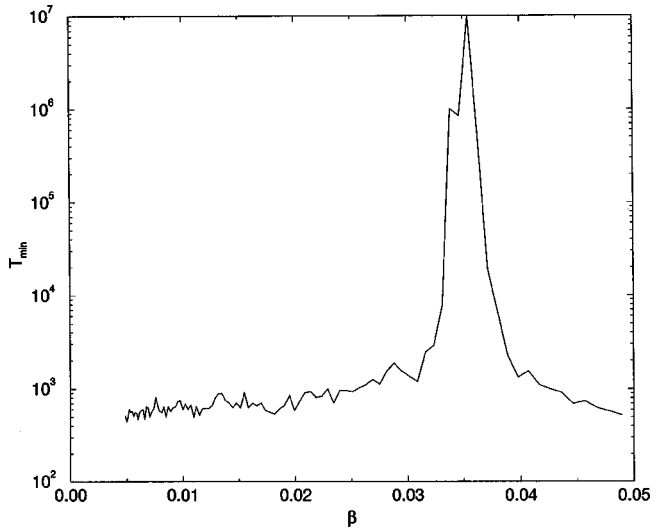

FIG. 6. Minimum time to ionization (among 24 random perturbations of average size β^2 added to the orbit of Fig. 1). β is the adimensional parameter and time is measured in the scaled units of Sec. III.

tion of electrodynamics [6,10]. The Darwin equations of motion are a β^2 perturbation of the Coulomb dynamics, of size $\beta^2 \sim 10^{-4}$ for atomic energies. In the scaled units of Sec. II the Darwin Hamiltonian is the following β^2 perturbation of Hamiltonian (1):

$$\hat{\mathbf{H}}_D = \frac{1}{2}(|\vec{p}_1|^2 + |\vec{p}_2|^2) + \zeta(Z)\left\{\frac{1}{r_{12}} - \frac{Z}{r_1} - \frac{Z}{r_2}\right\} - \frac{\zeta(Z)\beta^2}{2r_{12}}[\vec{p}_1 \cdot \vec{p}_2 + (\hat{n}_{12} \cdot \vec{p}_1)(\hat{n}_{12} \cdot \vec{p}_2)] - \frac{\beta^2}{8}[|\vec{p}_1|^4 + |\vec{p}_2|^4], \quad (4)$$

where $\hat{n}_{12} \equiv (\vec{x}_1 - \vec{x}_2)/r_{12}$. The second line represents the Biot-Savart magnetic interaction plus the first relativistic correction to the static electric field and the last line describes the relativistic mass correction. Notice that these are both proportional to the small parameter β^2, which makes them a small scale-dependent perturbation on the scale-invariant Coulomb Hamiltonian (first line). It is possible to regularize the Darwin equations with the same double-Kustanheimo transformation [23], only that here one needs to define the regularized time using the higher powers $dt = r_1^2 r_2^2 ds$, instead of the lower powers $dt = r_1 r_2 ds$ used to regularize the Coulomb equations [23].

The main question we address numerically in this section is the dependence of the stability of a nonionizing orbit with the energy scale of the orbit. Here we use the word stability to mean ionization stability: We call an initial condition ionization stable if any small perturbation of it produces another nonionizing orbit. The scale-dependent Darwin terms (of size β^2) produce significant deviations from the Coulomb dynamics only in a time scale of order $1/\beta^2$, which we find numerically to be the typical time for a nonionizing Coulombian initial condition to ionize along the Darwin vector field. This poses a numerical difficulty if β is too small because one has to integrate the orbit for very long times to investigate the stability. Numerical experiments taught us that ionization-stable orbits can be found at larger values of β for larger values of Z. This dynamical stability mechanism was first suggested by quantum atomic physics, where the values of β vary with the nuclear charge as $\beta \sim Z/137$. Large values of Z facilitate the numerical procedure and in the following we present the numerical investigation of the stability of nonionizing orbits starting from the large Z case.

Let us start with the $Z=20$ calcium ion two-electron system along the nonionizing orbit of Fig. 1 by fixing $r_1 = 1.4$ and $v_1 = 1.284\,42$ in the condition defined in Sec. III. To test the stability of the orbit at each value of β we add a random perturbation of average size β^2 to the initial condition and integrate the Darwin dynamics until either we find ionization or the time of integration is greater than 10^7 time units. We repeat this for at least 12 randomly chosen perturbations (because of the 12 degrees of freedom) and the minimum time to ionization is plotted in Fig. 6 as a function of β. It can be seen that only for a narrow set of values around $\beta \sim 0.037$ was this minimum time to ionization greater than 10^6. For the other values it decreases rapidly to a value of about 10^3. One could argue that for the other values of β the nonionizing initial condition has shifted away from the $v_1 = 1.284\,42$ initial condition, this being the reason that our orbit ionized. To test this, we fixed β at a ''bad'' value, for example, $\beta = 0.02$, and varied the plane initial condition in the β^2 neighborhood of this condition of Fig. 1 (we tried some 10 000 different values). We found that the minimum time to ionization was always about 10^3. Even the maximum time before ionization was about 10^4. We also searched in a bigger neighborhood, of size proportional to β, but the minimum time to ionization remained at 10^3 as well as the maximum at 10^4 for all tries. This suggests an interpretation that for the special resonant value of $\beta = 0.037$ the net diffusive effect of the scale-dependent term vanishes, allowing a nonionizing perturbed manifold. If the nonionizing initial condition had simply shifted away, at least one of the thousands of tries would get close to it and the maximum time among all tries would signal it. In order to have a direct reading (in atomic units) of the scale parameter β, we scaled to -1 the

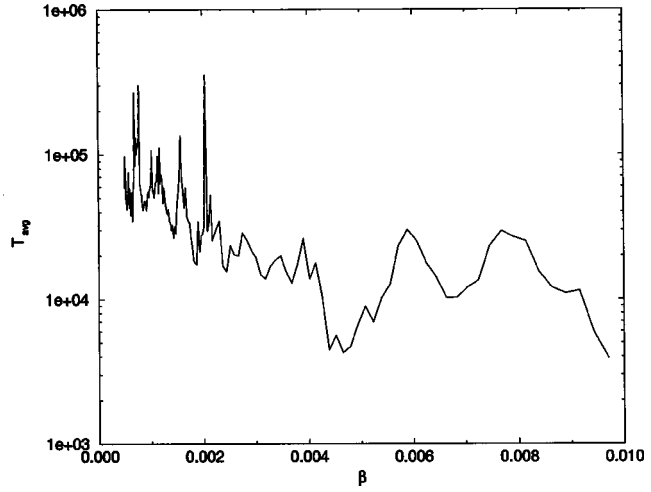

FIG. 7. Average time to ionization (among 12 random perturbations of average size $20\beta^2$ added to the orbit of Fig. 3). β is the adimensional scale parameter and time is measured in the scaled units of Sec. III.

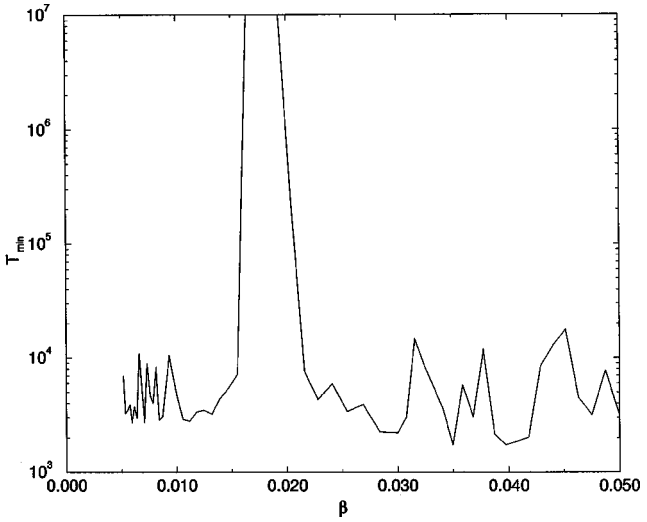

FIG. 8. Minimum time to ionization (among 24 random perturbations of average size β added to the orbit of Fig. 4). β is the adimensional parameter and time is measured in the scaled units of Sec. III.

energy of the initial condition of Fig. 1 before the numerical work (by use of the Coulombian scale invariance). Then, by use of Eq. (2), the energy of the orbit in ergs is given by $E = mc^2\beta^2\hat{H} = -mc^2\beta^2$, and for $\beta = 0.037$ this is approximately -24.59 a.u. The total angular momentum of this orbit is $l_z = 7.94\hbar$. This orbit's energy is above the ionization continuum of the ion, $E = -mc^2\alpha^2Z^2/2 = -200$ a.u., but it is still in the quantum range. It serves nevertheless to demonstrate that this dynamical system might exhibit nonionizing stable orbits only at very sharply defined energy values.

For the orbits of Figs. 2 and 3, the above procedure becomes prohibitively slow, as the value of β are much smaller and one must integrate for very long times, much beyond the estimated shadowing time. To partially overcome this we used a larger amplitude random perturbation (of average size $20\beta^2$), to produce faster ionization. The drawback with this is that the minimum ionization time does not show pronounced peaks; only the average ionization time still shows a signature of scale dependence. In Fig. 7 we show this average time for the orbit of Fig. 3. The peak value of $\beta = 0.002$ of Fig. 7 can be used with Eq. (2) to find the absolute value of the scaled sharp Fourier frequency $\hat{\omega} \simeq 1.75$ of Fig. 5, which for $\beta = 0.002$ is evaluated by Eq. (2) as 0.02 a.u. (infrared). The energy of the orbit for $\beta = 0.002$ is evaluated as $E = -mc^2\beta^2 = -0.15$ a.u., again a shallow level above the ionization threshold.

In Fig. 8 we show the minimum ionization time (among 24 random perturbations of size β), of the nonionizing orbit of Fig. 4. Notice that we used a much larger perturbation, of size proportional to β instead of β^2, as the stability island becomes larger for larger Z. The peak of the minimum ionization time also becomes wider for this large value of Z.

This property of sharply defined energies can possibly be found for the lower-lying energies below the ionization threshold as well. These orbits would involve configurations where the electrons come very close to the nucleus and acquire a large velocity. Even though our integrator is regularized, the correct physical electronic repulsion is greatly amplified when one electron has a relativistic velocity and the Darwin approximation cannot describe the physics then. For this above reason, we do not study the frozen-planet periodic orbit (the two electrons performing one-dimensional periodic motion on the same side of the nucleus, with the inner electron rebounding from the origin, an artifact of regularization). The Darwin approximation would fail again, as the inner particle goes to the speed of light. There would also be some numerical-regularization difficulties involved if one wanted to study this dynamical system anyway. The correct relativistic ''froze-planet'' dynamics can actually produce a new *physical* inner turning point very close to the origin but not *at* the origin as the regularized motion, and we discuss this elsewhere [30]. Here we shall be contempt with these interesting results for the shallow orbits already.

Last, we consider the nonionizing symmetric periodic orbit called the Langmuir orbit, where the two electrons perform symmetric bending motion shaped approximately like a semicircle [28]. For the Coulomb two-electron atom with $Z = 2$ this orbit was found to have a zero maximum Lyapunov exponent [25]. The orbit is therefore neutrally stable, which is the best one can expect from a periodic orbit of a Hamiltonian vector field. (Absolute stability violates the symplectic symmetry, which says that to every stability exponent λ one should have a $1/\lambda$ exponent.) It is a simple matter to obtain the Langmuir-like orbit for the Darwin Hamiltonian at any given value of β: all it takes is a little adjusting in the neighborhood of the Coulombian Langmuir condition. We attempted to investigate numerically any scale-dependent diffusion away from this Darwin-Langmuir condition for β in the atomic range, but again the numerics is prohibitively slow at the time of writing this work. It is known from modern perturbation theory that Arnold diffusion in the presence of resonances can be much slower, and we refer the reader to the ''stability by resonance results'' [31,32].

V. CONCLUSIONS AND DISCUSSION

The simplified dynamical mechanism behind resonant nonionization seems to go intuitively as follows: The pecu-

liar scale-invariant Coulomb dynamics determines the nonionizing orbits within narrow ''stochastic tubes.'' The next step is the action of the small scale-dependent relativistic corrections that produce a slow diffusion of the orbit out of the thin tube in a time of the order of $1/\beta^2$. After this, quick ionization follows. Only at very special resonant values of β do the relativistic terms leave the orbit within the tube, a resonant effect that depends on β, fixing the energy scale. In Ref. [3], it was shown that at least one nonionizing plane Coulombian orbit is found in the center of four resonance islands in a ''four-surface of section'' of the four-degree-of-freedom Hamiltonian (Figs. 15, 16, and 17 of Ref. [3]). For the general higher-dimensional complex orbits we studied, we could not find a fortunate way to project those islands, but of course our ''stochastic tubes'' should be stochastic resonance islands. In the literature, the escape to infinity from simpler-to-understand two-degree-of-freedom systems has been attributed to cantori, which, as is well known, can trap chaotic orbits near regular regions for extremely long times [5]. In the present larger dimensional case it appears that resonances are also controlling the escape to infinity of one electron by the existence of extra resonant constants of motion [6,7]. This seems to be in agreement with the numerical results of very sharp peaks for the minimum ionization time and also with the ''stability by resonance'' results [31,32]. We have tried to concentrate on the physics described by this combination of chaotic dynamics on a two-electron atom with inclusion of relativistic correction, while discussing this highly nontrivial result of nonlinear dynamics.

In Refs. [6,7] we noticed that a simple resonant normal form criterion gives a surprisingly good prediction for the discrete atomic energy levels of helium. The resonant structure was calculated using the Darwin interaction (4), which is the low-velocity approximation to both Maxwell's [6,7] and Wheeler-Feynman's [8] electrodynamics. As we saw in Sec. III, the Coulombian nonionizing orbits are far from circular, and these orbits would radiate even in dipole according to the time-irreversible Maxwell's electrodynamics (circular orbits radiate only in quadrupole but are linearly unstable). It becomes then clear that the heuristic results of [6,7] have a simpler physical meaning in the context of a time-reversible direct-interaction theory (as the action-at-a-distance electrodynamics for example).

The combination of chaotic dynamics with relativistic invariance has never been explored numerically, and most known Lorentz-invariant dynamical systems are for one particle and possess trivially integrable dynamics. The situation gets unexpectedly much more complicated for more than one particle (apart from the trivial noninteracting many-particle system): Due to the famous no-interaction theorem [29], the relativistic description of two directly interacting particles is impossible within the Hamiltonian formalism and its set of ten canonical generators for the Poincaré group [20]. A description of interacting particles is possible only in the context of constraint dynamics, with 11 canonical generators and with covariantly defined Dirac brackets replacing the Poisson brackets. The interested reader should consult some recently found two-body direct-interaction relativistic Lagrangian dynamical systems [17] as well as the constraint-dynamics direct-interaction models recently used in chromodynamics and two-body Dirac equations [18–21]. The nonlinear dynamics of these models could display the same type of interesting dynamical behavior.

It would be natural to wonder if one can find an analogous scale-dependent dynamics for a dynamical system describing the hydrogen atom, apparently the simplest example of Lorentz-invariant two-body relativistic dynamics of atomic interest. It turns out that hydrogen is not simpler than helium at all, but it appears to us that there is an essential difference which has actually made the interesting dynamics of a two-electron atom amenable to study already within the Darwin approximation: In a two-electron atom orbits with a negative energy can ionize, while in hydrogen this might be possible only if one includes several correction orders of the relativistic action-at-a-distance interaction. (For instance, this will bring stochasticity to the simple planetary Coulombian hydrogen.) Ionization with a negative energy would be impossible for hydrogen within the Darwin approximation (unless the electron goes to the speed of light). This is an indication that in hydrogen the essential physics described by the action-at-a-distance electrodynamics is of nonperturbative character. The paradoxical result of the infinite linear instability of circular orbits in atomic hydrogen [33] is another warning of this nonperturbative dynamics.

ACKNOWLEDGMENTS

The author acknowledges the support of FAPESP, process 96/06479-9, and CNPQ, process 301243/94-8(NV).

[1] Z. Xia, J. Diff. Eqns. **110**, 289 (1994).
[2] T. Yamamoto and K. Kaneko, Phys. Rev. Lett. **70**, 1928 (1993).
[3] T. Yamamoto and K. Kaneko, Prog. Theor. Phys. **100**, 1089 (1998).
[4] S. Bleher, C. Grebogi, E. Ott, and R. Brown, Phys. Rev. A **38**, 930 (1988); F. T. Arecchi, R. Badii, and A. Politi, *ibid.* **32**, 402 (1985); F. C. Moon and G.-X. Li, Phys. Rev. Lett. **55**, 1439 (1985); E. G. Gwinn and R. M. Westervelt, *ibid.* **54**, 1613 (1985); C. Grebogi, S. McDonald, E. Ott, and J. Yorke, Phys. Lett. **99A**, 415 (1983).
[5] H. Kandrup, C. Siopis, G. Contopoulos, and R. Dvorak, Chaos **9**, 381 (1999).
[6] J. De Luca, Phys. Rev. Lett. **80**, 680 (1998).
[7] J. De Luca, Phys. Rev. E **58**, 5727 (1998).
[8] J. L. Anderson, *Principles of Relativity Physics* (Academic, New York, 1967), p. 225.
[9] R. N. Hill, *Relativistic Action at a Distance: Classical and Quantum Aspects, Proceedings, Barcelona, Spain, 1981*, edited by J. Llosa, Lecture Notes in Physics Vol. 162 (Springer, New York, 1982), p. 104.
[10] H. W. Woodcock and P. Havas, Phys. Rev. D **6**, 3422 (1972).
[11] V. Mehra and J. De Luca, Phys. Rev. E **61**, 1199 (2000).
[12] J. A. Wheeler and R. P. Feynman, Rev. Mod. Phys. **17**, 157 (1945); **21**, 425 (1949).
[13] D. Leiter, Am. J. Phys. **38**, 207 (1970).

[14] G. N. Plass, Ph.D. thesis, Princeton University, 1946 (unpublished).
[15] P. A. M. Dirac, Proc. R. Soc. London, Ser. A **167**, 148 (1938).
[16] A. Einstein and W. Ritz, Phys. Z. **10**, 323 (1909).
[17] R. P. Gaida, V. Tretyak, and Yu. Yaremko, e-print physics/9812107; A. Duviryak, V. Shpytko, and V. Tretyak, e-print physics/9812125.
[18] H. Crater and Dujiu Yang, J. Math. Phys. **32**, 2374 (1991).
[19] H. W. Crater and P. Van Alstine, Phys. Rev. D **46**, 766 (1992).
[20] *Proceedings of the Workshop held in Firenze, Italy, 1986*, edited by G. Longhi and L. Lusanna (World Scientific, Singapore, 1987).
[21] H. Crater and L. Lusanna, e-print physics/0001046.
[22] J. H. Verner, SIAM (Soc. Ind. Appl. Math.) J. Numer. Anal. **15**, 772 (1978).
[23] S. J. Aarseth and K. Zare, Celest. Mech. **10**, 185 (1974).
[24] T. Sauer, C. Grebogi, and J. A. Yorke, Phys. Rev. Lett. **79**, 59 (1997).
[25] K. Richter and D. Wintgen, J. Phys. B **23**, L197 (1990); , Phys. Rev. Lett. **65**, 1965 (1990); K. Richter, G. Tanner, and D. Wintgen, Phys. Rev. A **48**, 4182 (1993); D. Wintgen, A. Bürgers, K. Richter, and G. Tanner, Prog. Theor. Phys. Suppl. **116**, 121 (1994).
[26] A. Lopez-Castillo, M. A. M. de Aguiar, and A. M. Ozorio de Almeida, J. Phys. B **29**, 197 (1996).
[27] P. Gaspard and S. Rice, Phys. Rev. A **48**, 54 (1993); E. Cravo and A. C. Fonseca, Few-Body Syst. **5**, 117 (1988).
[28] J. Müller, J. Burgdörfer, and D. Noid, Phys. Rev. A **45**, 1471 (1992).
[29] D. G. Currie, T. F. Jordan, and E. C. G. Sudarshan, Rev. Mod. Phys. **35**, 350 (1963); also in *The Theory of Action-at-a-Distance in Relativistic Particle Dynamics*, edited by Edward H. Kerner (Gordon and Breach, New York, 1972).
[30] J. De Luca and V. Mehra (unpublished).
[31] G. Bennetin, L. Galgani, and A. Giorgilli, Commun. Math. Phys. **121**, 557 (1989).
[32] P. Lochak, Nonlinearity **6**, 885 (1993).
[33] C. M. Andersen and H. C. Von Baeyer, Phys. Rev. D **5**, 802 (1972). The sign of the acceleration terms in Eq. (2.3) of this paper is wrongly calculated and we do not know if it affects the stability results.